CrystEngComm

Accepted Manuscript

ROYAL SOCIETY OF CHEMISTRY

www.rsc.org/crystengcomm

CrystEngComm RSCPublishing

PAPER

Bio-Inspired Nacre-like Layered Hybrid Structure of Calcium Carbonate under the Control of Carboxyl Graphene

Cite this: DOI: 10.1039/xoxxoooooox

Received ooth January 2012,
Accepted ooth January 2012

DOI: 10.1039/xoxxoooooox

www.rsc.org/

Jie Li,[ab] Dandan Liu,[b] Bo Li,[b] Hao Wei,*[ab] Jun Wang,[ab] Shihui Han,[ab] and Lianhe Liu[ab]

In this paper, carboxyl graphene (GO-COOH) sheet matrices, which are heavily oxygenated and are similar to the organic matrices of molluscs, were used to construct nacre-like layered structures. The results showed that the surface of hybrids was smooth and the cross section had a multi-layer structure. Both the surface and the interlayer of the composite material generated calcium carbonate ($CaCO_3$) crystals. Furthermore, the spontaneity of the layered structure was found to be closely related to the concentration of $CaCO_3$ crystals in which high concentration could inhibit the process, highlighting the determining role of the $CaCO_3$ concentration. To better understand the mechanisms for the formation of the layered structure, scanning electron microscope (SEM), transmission electron microscope (TEM), X-ray diffraction (XRD), thermo-gravimetric analysis (TGA) and Fourier-transformed infrared spectrometry (FT-IR) were employed. This work represents an efficient and controllable way to construct of nacre-like layered hybrid structures and also has great potential for promoting the application of GO-COOH in biomedical engineering, especially in the biomimetic material fields.

Introduction

Natural biominerals, such as bone, teeth and the nacre of a shell, with high mechanical strength and toughness, have inspired scientists and researchers for decades.[1-3] In these biominerals, the properties are closely related to their hierarchically ordered layered structures. For instance, the nacre of a shell has a layered structure that is composed of approximately 95wt % $CaCO_3$ and 5wt % organic matrices,[4,5] which give rise to high mechanical strength[6]. In these processes, organic matrices, such as proteins and polysaccharides, play an important role in controlling the orientation, polymorphism, composition, and morphology of the mineral phase.[7-9] In recent years, many strategies have been developed to mimic the formation of biomineral hybrid material structures.[10-15] A variety of calcium-based hybrid materials have been reported.[16-21] It was previously reported the preparation of artificial nacre by alternating layer-by-layer polymer films and $CaCO_3$ strata, in our previous study.[22] These results showed that the cross-section of artificial nacre reveals a two or four layer structure and that the matrix is important for further structural control of inorganic/organic hybrid materials. However, the control over a multi-layer structure of $CaCO_3$ crystals biomineral hybrid materials is still a challenging task.

GO-COOH is a single-atom-thick sheet of 2-dimensional layers. The graphene-derived sheet in GO-COOH is heavily oxygenated, bearing carboxyl (-COOH) and hydroxyl (-OH) hydrophilic groups on their basal planes, which is similar to the organic matrices of mollusc shells. It was reported that organic matrices that contain –OH and -COOH to control which polymorph they use, the crystal face and orientation, and the particle shape and size in crystallization processes[23]. GO-COOH possibly represents an ideal mineralization matrix. To date, only a few studies have reported on the composite crystals of graphene oxide (GO) or graphene and $CaCO_3$. The self-standing GO/graphene–$CaCO_3$ hybrid films compose of vaterite microspheres that were wrapped and interconnected by GO (or graphene) networks were reported.[24] Composite crystals of $CaCO_3$ and graphene with hexagonal plate or ring, dendritic and rhombohedral shapes were synthesized by the hydrothermal reaction.[25] Furthermore, hybridization or interaction of GO-COOH with $CaCO_3$ crystals to control a layered structure has rarely been reported.

In our study, GO-COOH sheet matrices were used to induce mineralization of $CaCO_3$ crystals to biomimetically construct GO-COOH/$CaCO_3$ hybrid materials. First, $CaCl_2$ aqueous solution was slowly added dropwise into the GO-COOH dispersion solution without stirring (10 drops per minute) and then adjusted the pH value of the solution. Finally, Na_2CO_3 aqueous solution (Ca^{2+} and CO_3^{2-} were mixed in a 1:1 ratio during this step) was slowly added dropwise into the solution without stirring (10 drops per minute) and stewed for 24 h. The main advantage of the proposed method is the very slow process, to ensure the slow crystallization growth of $CaCO_3$ crystals in exfoliated GO-COOH nanosheet to fabricate a GO-COOH/$CaCO_3$ layered hybrid structure. It is anticipated that

this line of research may provide an efficient and controllable way for fabricating nacre-like layered hybrid structure.

Experiment section

Materials.

Anhydrous calcium chloride, sodium carbonate and sodium hydroxide were purchased from Sinopharm Chemical Reagent Co., Ltd. (Shanghai, China) and were of analytical grade. Carboxyl graphene dispersion (diameter > 500 nm, thickness 0.8~1.2 nm, single layer ratio≈80%, purity≈99.8wt%, carboxyl ratio 5%) was purchased from Nanjing XFNANO Materials Tech Co., Ltd. (Nanjing, China). Aqueous solutions of $CaCl_2$ (> 96.0%), Na_2CO_3 (> 99.8%) and NaOH (> 96.0%) were prepared just before use. The purified water used in this study was prepared with Milli-Q Plus system (Millipore) and had a relative resistivity higher than 18.0 MΩ cm.

Preparation.

GO-COOH was dispersed in aqueous solution (2.0 mg mL^{-1}, 20.0 mL) under ultrasonication for 3h. Next, 20mL of a 4mM $CaCl_2$ aqueous solution was slowly added dropwise into the GO-COOH dispersion solution without stirring (10 drops per minute). 0.1 M NaOH adjusted the pH value of the solution to 6.80, which was then ultrasonicated for 1h. Then, 40mL of a 2mM Na_2CO_3 aqueous solution (Ca^{2+} and CO_3^{2-} were mixed in a 1:1 ratio during this step) was slowly added dropwise into the solution without stirring (10 drops per minute) and stewed for 24 h. All experiments were conducted at room temperature. The mixture was washed by repeated centrifugation, first with distilled water and then absolute ethyl alcohol, and dried at 40 ℃ in a vacuum for 24 h. The main method is to set up a very slowly process, in order to ensure that the slowly crystallization growth of $CaCO_3$ crystals in the exfoliated GO-COOH nanosheet.

Characterization.

The samples were Au-coated prior to examination by a QUANTA 200 scanning electron microscope (SEM), operating at an accelerating voltage of 15 kV. X-ray diffraction (XRD) measurements were conducted using a Rigaku TTR-III powder X-ray diffractometer with Cu Kα radiation (λ=0.15406nm, 40 kV, 120 mA), and 0.02° step and 2θ range of 5-60° were selected to analyze the crystal structure. The samples were placed onto carbon mesh grids (200 mesh) for transmission electron microscopy (TEM) and high-resolution transmission electron microscopy (HRTEM) imaging (JEM-2200FS) at an accelerating voltage of 200 kV. FT-IR spectroscopic measurements were performed on a PE100 FT-IR spectrometer (America), with scanning number of 16 and resolution of 4 cm^{-1}. The samples were tested by thermogravimetric analysis (TGA) using a TQ50 TGA analyzer, purged with nitrogen gas.

Results and discussion

Fig. 1 shows the SEM images of GO-COOH/$CaCO_3$ hybrids obtained after 24 h of stewing. SEM observation of the hybrids reveals a layered structure similar to that of abalone shell.[26,27] The low magnified image of GO-COOH/$CaCO_3$ hybrid material (Fig. 1a) shows five pieces that possess a smooth surface and an overall multilayered structure.

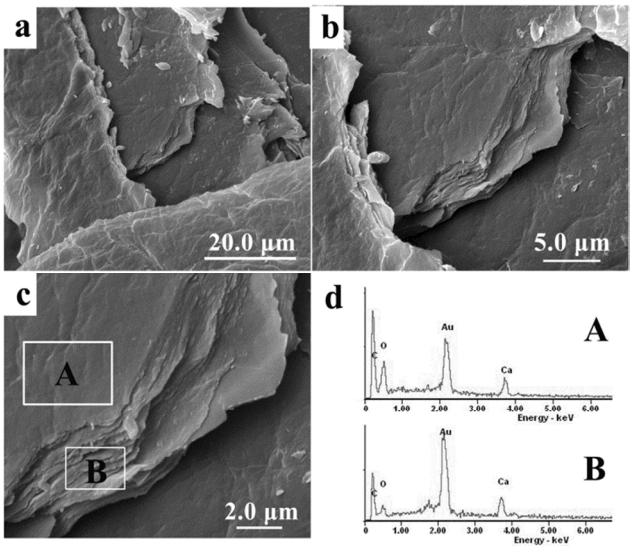

Fig. 1 SEM images of GO-COOH/$CaCO_3$ hybrid materials: a) low magnification SEM image, b) and c) high magnification SEM images of a), d) SEM-EDXA spectra, (A) and (B) shown in panel (c).

The section of a high magnified SEM image (Fig. 1b, Fig. 1c) indicates the multilayer structure more clearly with thin-films stacked, which was different from GO-COOH aqueous solution after dried in same method (Fig. S1) and GO films[28]. To determine the reason for this observation, we conducted a series of characterizations. The elemental compositions of sites A and B in the magnified regional SEM image (Fig. 1c) were analyzed by SEM with elemental distribution analysis (SEM-EDAX, Fig. 1d). The atomic ratios of C, O and Ca of sites A and B were calculated to be 67: 29: 4 and 7: 2: 1, respectively. This suggested that both the surface and the interlayer of the composite material generated $CaCO_3$ crystals.

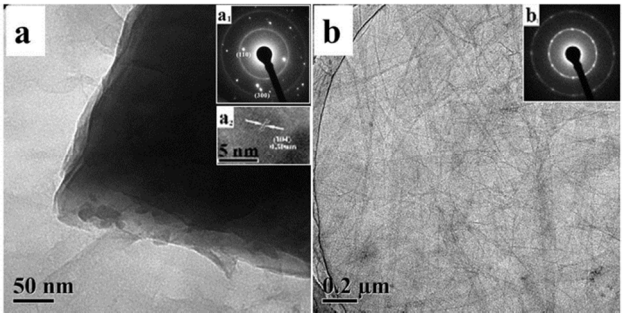

Fig. 2 Bright-field transmission electron microscopy (TEM) images of a) GO-COOH/$CaCO_3$ hybrid material and b) GO-COOH, corresponding-selected area electron diffraction (SAED) pattern (inset a_1 and b_1), the inset of (a_2) is the high-resolution transmission electron microscopy (HRTEM) of the GO-COOH/$CaCO_3$ hybrid material.

The bright-field TEM image and the corresponding selected-area of electron diffraction patterns (SAED) are presented in Fig. 2. TEM image of GO-COOH/$CaCO_3$ hybrid material (Fig. 2a) shows a stacking of layered structure. The SAED pattern of GO-COOH/$CaCO_3$ hybrid material (inset a_1) reveals new crystal formation in addition to an amorphous concentric ring structure of GO-COOH. The diffraction spot in the SAED pattern is indexed as the (110) and (300) diffractions of the

calcite crystal of $CaCO_3$, displaying a polycrystalline structure.[29] The HRTEM image of the hybrids provides further insights into the nanostructure, as shown in Fig. a_2. The distances between the lattice fringe of the particles are around 3.0 Å, which correspond to the d spacing of the (104) planes of the $CaCO_3$ calcite crystal, confirming the formation of $CaCO_3$ crystals, which is consistent with the XRD result. The GO-COOH large layers between grid lines are clearly observed in Fig. 2b. The SAED pattern of GO-COOH (inset of b_1) shows an amorphous concentric ring structure. This indicates that GO-COOH is highly oxidized.[30] These observations suggest that the GO-COOH matrix induces crystallization of $CaCO_3$ crystals to form a layered structure.

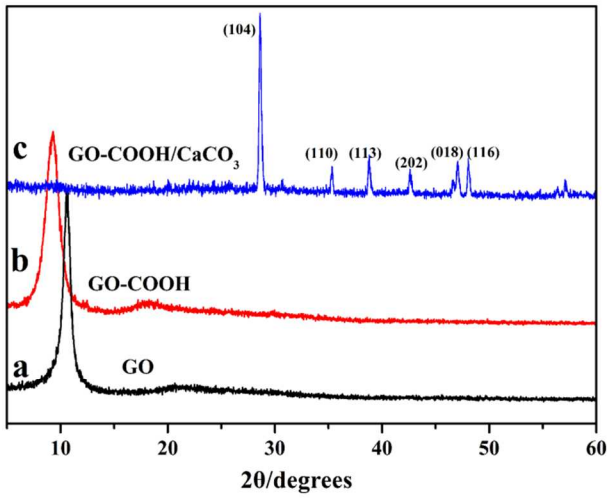

Fig. 3 Typical XRD diffraction patterns of GO, GO-COOH and the GO-COOH/$CaCO_3$ hybrid materials.

To prove the laminated structure of the GO-COOH/$CaCO_3$ hybrid materials, XRD patterns (Fig. 3) of GO, GO-COOH and the $CaCO_3$/GO-COOH hybrids were characterized. The diffraction peak of exfoliated GO (Fig. 3a) at 10.6° (001) features a basal spacing of 0.83 nm, showing the complete oxidation of graphite to GO due to the introduction of oxygen-containing functional groups onto the graphite sheet.[31] In the XRD pattern of GO-COOH (Fig. 3b), the diffraction peak located at 9.4° is smaller than the diffraction peak of GO, revealing that GO-COOH has a larger spacing compared with GO. The XRD pattern of the hybrids (Fig. 3c) displays have a very weak diffraction peaks (2θ [°]) of GO-COOH and those of the $CaCO_3$ calcite crystals. The diffraction peak of GO-COOH almost disappeared, since the regular stacks of GO-COOH sheets were exfoliated.[32] The diffraction peaks of calcite are 29.400, 35.968, 39.408, 43.157, 47.504, and 48.503, which correlated to the (hkl) indices (104), (110), (11$\bar{3}$), (202) (018), and (11 $\bar{6}$), respectively. As shown in the typical XRD diffraction patterns of pure $CaCO_3$ crystals in aqueous solution after 24 h of reaction (Fig. S2), (hkl) indices (012), (104), (110), (11$\bar{3}$), (202) (018), and (11$\bar{6}$), respectively. This indicates that the existence of the GO–COOH is inhibited the (012) formation of $CaCO_3$ calcite crystals. It was found that the diffraction peaks of the layered structure do not appear in the hybrid materials, because the layer spacing and lamellar structure are beyond XRD measurement range.

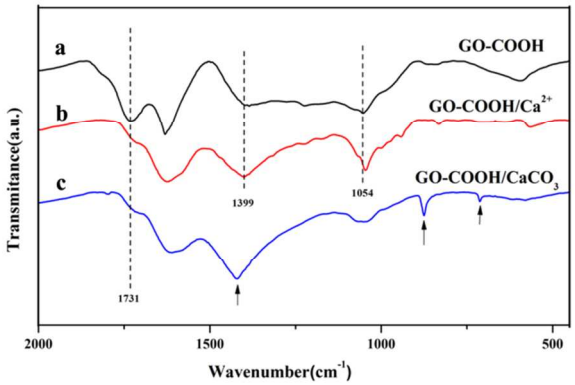

Fig. 4 Fourier-transformed infrared spectrometry (FT-IR) of GO-COOH, GO-COOH/Ca^{2+} and GO-COOH/$CaCO_3$.

To further investigate the effects of GO-COOH on the mineralization of $CaCO_3$ crystals, we analyzed the time-dependent phase transitions of $CaCO_3$ precipitates using FT-IR spectroscopy. GO-COOH and the multi-layer structure of GO-COOH/$CaCO_3$ hybrids material were verified by characteristic vibration bands of FT-IR spectroscopy. As shown in Fig. 4, the absorption bands at 1731 and 1399/1054 cm^{-1} are ascribed to the C=O stretching of the –COOH and the C–/O stretching of the C–OH/C–O–C groups, respectively.[33,34] In the middle of the experimental process, we obtain GO-COOH /$CaCl_2$ hybrids with the only addition of $CaCl_2$. Compared to GO-COOH, the sample of GO-COOH/$CaCl_2$ has weaker C=O stretching absorption (Fig. 4b), indicating that when Ca^{2+} is added the environment of carboxyl groups changes. After the introduction of CO_3^{2+} further mineralization generates crystalline $CaCO_3$ crystals. Identification of the GO-COOH/$CaCO_3$ hybrid material is also verified by the characteristic vibration bands in FT-IR spectroscopy, 1425, 874, 712 cm^{-1} for calcite of $CaCO_3$ crystals.[35] (Fig. 4c)

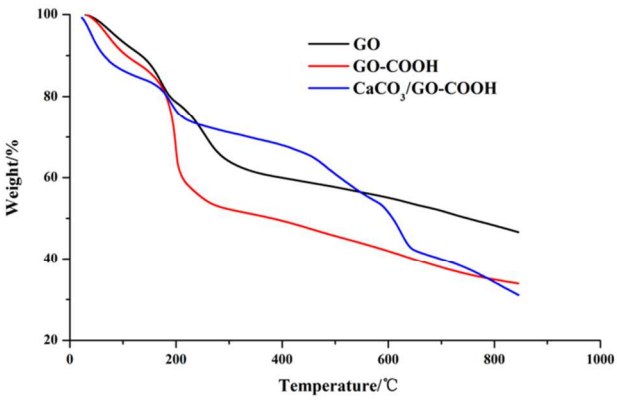

Fig. 5 Thermogravimetric analysis(TGA) of GO, GO-COOH and GO-COOH/$CaCO_3$.

TGA was employed to determine the weight content of organic and inorganic material in GO-COOH/$CaCO_3$ hybrid materials. As shown in Fig. 5, the weight loss of GO (the black line) is approximately 19% (from room temperature to 178 ℃), which indicates the amount of evaporation of adsorbed water and bound water. When the temperature rises to 312 ℃, a sharp reduction in the amount quality of GO by 20 %, is attributed to

the decomposition of hydroxyl groups, epoxy and carboxyl oxygen-containing functional groups on the surface of the GO, affecting the quality The weight loss of GO-COOH (the red line) and the COOH/$CaCO_3$ hybrid materials (the blue line) are similar to GO from room temperature to 178 ℃. It means that they have same content of adsorbed and bound water[36]. But from 178 to 312 ℃, the weight loss in GO-COOH is about 30 % far more than the weight loss of GO. It means that the content of oxygen containing functional groups in GO-COOH is higher than GO. The weight loss is about 9.5 % from 178 to 312 ℃ in GO-COOH/$CaCO_3$ hybrid materials (the blue line), which is attributed to the decomposition of oxygen functional groups in GO-COOH films. Further increase of temperature results in the decomposition of $CaCO_3$ crystals in hybrid materials, and at 627 ℃ decomposition becomes stronger.[37,38] By comparison, the mass fraction of $CaCO_3$ crystals in the hybrid materials is calculated to be 68.3%.

To confirm the relationship between $CaCO_3$ concentration and microcosmic multi-layers structure, we carried out an experiment using different concentrations of $CaCO_3$. The SEM results shown in Fig. 6a and 6d suggest the type of morphology of $CaCO_3$ at a concentration of 5 mM. The high magnification SEM image (Fig. 6d) indicates a nacre-like layered structure. When the concentration of $CaCO_3$ increased to 10 mM (Fig. 6b and 6e), rhombohedral $CaCO_3$ calcite crystals form between GO-COOH sheets. With a further increase of the concentration of $CaCO_3$ to 100 mM (Fig. 6c and 6f), $CaCO_3$ crystals transform into individual diamond crystal, whereas GO-COOH attaches to the surface of $CaCO_3$ crystals in a facile manner. This result shows that when the concentration of $CaCO_3$ increases, the growth of calcite of crystalline $CaCO_3$ proceeds more vigorously. When the concentration of $CaCO_3$ is less than 5mM, GO-COOH successfully controls the growth of $CaCO_3$ crystals to construct a layered structure. The fabrication of GO-COOH/$CaCO_3$ layered structure was closely related to the concentration of $CaCO_3$ crystals in which high concentration could inhibit the process, highlighting the determinant of $CaCO_3$ concentration.

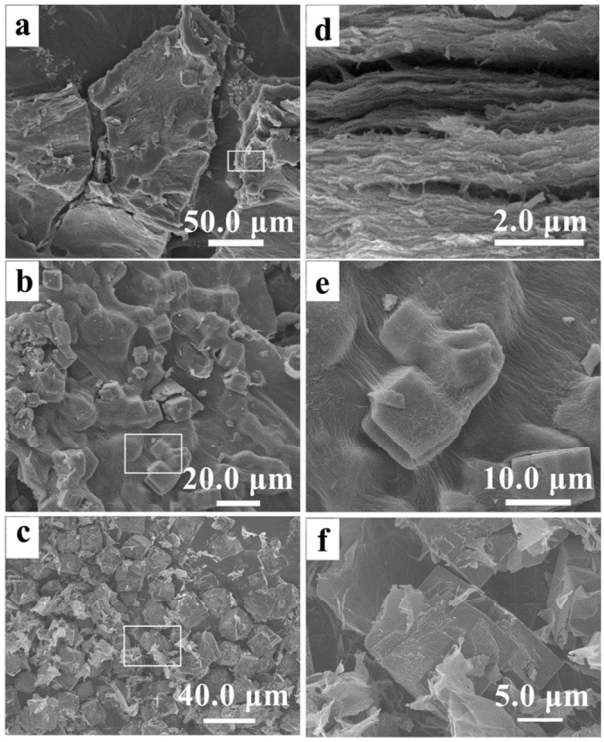

Fig. 6 SEM images of the GO-COOH/$CaCO_3$ hybrid materials in different consistence of $CaCO_3$: (a)-(c) 5, 10, 100mM; (d) - (f) high magnification SEM images of (a)-(c), respectively.

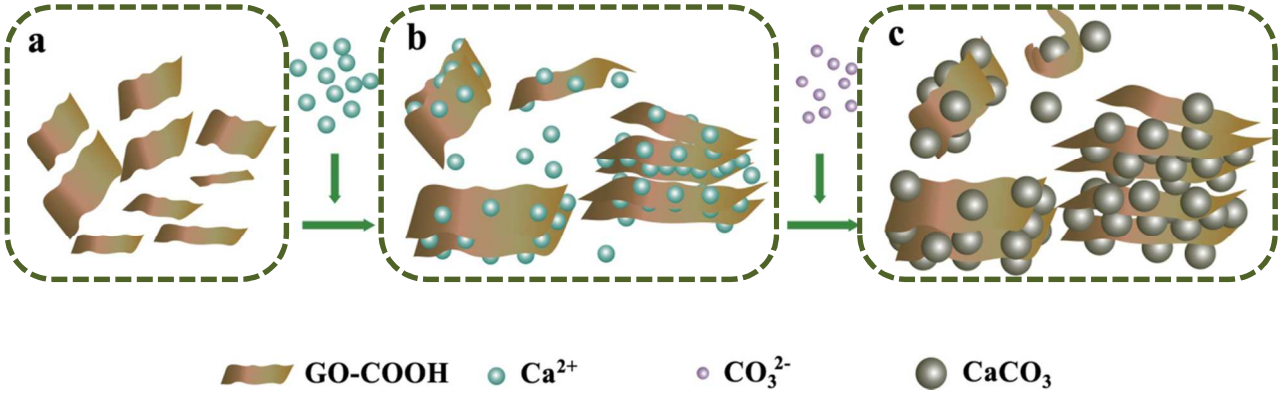

Fig. 7 Schematic illustration for the fabrication of GO-COOH/$CaCO_3$ multi-layer structure: (a) GO-COOH nanosheet in aqueous solution; (b) addition of $CaCl_2$ and formation of GO-COOH /$CaCl_2$ hybrid multi-layer structure; (c) addition of Na_2CO_3 and formation of GO-COOH /$CaCO_3$ hybrid multi-layer structure.

It is speculated that the fabrication of GO-COOH/$CaCO_3$ multi-layer materials were involves three steps, as illustrated in fig. 7: (a) GO-COOH nanosheet is dispersed in aqueous solution (Fig. 7a). (b) $CaCl_2$ is added to form the GO-COOH/$CaCl_2$ hybrid multi-layer structure. Compared to the GO-COOH, the sample GO-COOH/$CaCl_2$ has weaker C=O stretching absorption in FT-IR (Fig. 4), indicating that when Ca^{2+} is added the nature of carboxyl groups changes. It was conjectured that Ca^{2+} has a strong adherence for carboxyl groups on the surface of the GO-COOH. SEM observation (Fig. S3) of the cross section of GO-COOH/$CaCl_2$ hybrids reveals a loose multilayered structure. After the introduction of CO_3^{2-} further generation of mineralized crystalline $CaCO_3$ crystals in the film space of GO-COOH. (c) Na_2CO_3 is added to form the GO-COOH/$CaCO_3$ hybrid multi-layer structure. It was speculated that after the introduction of CO_3^{2+} further

generation of mineralized crystalline $CaCO_3$ occurs, which is consistent with the XRD and FT-IR results.

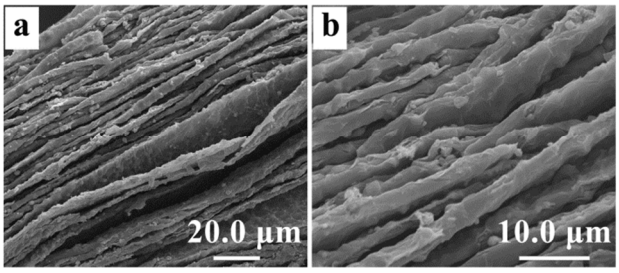

Fig. 8 SEM images of the GO-COOH/$BaSO_4$ hybrid materials: (b) high magnification SEM images of (a), respectively.

To prove the universal applicability of the method, $BaSO_4$ crystals were used rather than $CaCO_3$ crystals to carry out the same experiment. The results were shown in Fig. 8, SEM observation of the GO-COOH/$BaSO_4$ hybrid materials reveals a layered structure similar to that of GO-COOH/$CaCO_3$ hybrids. The high magnified SEM image (Fig. 8b) indicates the multilayer structure more clearly with globular $BaSO_4$ crystals.

Conclusions

In conclusion, GO-COOH is similar to the organic matrices of mollusk shells and it was speculated as an ideal mineralization matrix. In this study, we used GO-COOH sheet matrices to induce $CaCO_3$ crystals mineralization constructing the GO-COOH/$CaCO_3$ hybrid structure. The characterization techniques revealed that $CaCO_3$ crystals were successfully grafted onto exfoliated GO-COOH nanosheet and a microcosmic simulation of a multi-layer shell structure was successfully performed. The spontaneity of the layered structure was found to be closely related to the concentration of $CaCO_3$ crystals in which a high concentration could inhibit the process, highlighting the determinant of the $CaCO_3$ concentration. It is greatly anticipated that this work could represent an efficient and controllable way to construct of nacre-like layered hybrid structure and also has great potential to promote the application of GO-COOH in biomedical engineering, especially in the biomimetic material fields.

Acknowledgements

This work was supported by National Natural Science Foundation of China (51003018), Special Program for International S&T Cooperation Projects of China (2011DFR50770).

Notes and references

[a] Key Laboratory of Superlight Material and Surface Technology of Ministry of Education, College of Material Science and Chemical Engineering, Harbin Engineering University, Harbin 150001, PR China.
[b] Institute of Advanced Marine Materials, Harbin Engineering University, Harbin 150001, PR China.

1 L. Addadi and S. Weiner, *Angew. Chem., Int. Ed. Engl.*, 1992, **31**, 153-169.
2 T. Takeshita, Y. Matsuura, S. Arakawa and M. Okamoto, *Langmuir*, 2013, **29**, 11975-11981.
3 M. Vinoba, M. Bhagiyalakshmi, A. N. Grace, D. H. Chu, S. C. Nam, Y. Yoon, S. H. Yoon and S. K. Jeong, *Langmuir*, 2013, **29**, 15655-15663.
4 L. Addadi, D. Joester, F. Nudelman and S. Weiner, *Chem.-Eur. J.*, 2006, **12**, 980-987.
5 M. Suzuki, K. Saruwatari, T. Kogure, Y. Yamamoto, T. Nishimura, T. Kato and H. Nagasawa, *Science*, 2009, **325**, 1388-1390.
6 Q. F. Cheng, L. Jiang and Z. Y. Tang, *Acc. Chem. Res.*, 2014, **47**, 1256-1266.
7 F. C. Meldrum, *Int. Mater. Rev.*, 2003, **48**, 187-224.
8 A. S. Schenk, B. Cantaert, Y.-Y. Kim, Y. Li, E. S. Read, M. Semsarilar, S. P. Armes and F. C. Meldrum, *Chem. Mater.*, 2014, **26**, 2703-2711.
9 J. Shi, S. Zhang, X. Wang, C. Yang and Z. Jiang, *J. Mater. Chem. B.*, 2014, **2**, 4289-4296.
10 T. Kato, *Adv. Mater.*, 2000, **12**, 1543-1546.
11 A. Sugawara, T. Ishii and T. Kato, *Angew. Chem. Int. Ed.*, 2003, **42**, 5299-5303.
12 T. Sakamoto, A. Oichi, A. Sugawara and T. Kato, *Chem. Lett.*, 2006, **35**, 310-311.
13 C. Tian, C. Zhang, H. Wu, Y. Song, J. Shi, X. Wang, X. Song, C. Yang and Z. Jiang, *J. Mater. Chem. B.*, 2014, **2**, 4346-4355.
14 T. Sakamoto, A. Oichi, Y. Oaki, T. Nishimura, A. Sugawara and T. Kato, *Cryst. Growth Des.*, 2008, **9**, 622-625.
15 B. Cantaert, A. Verch, Y.-Y. Kim, H. Ludwig, V. N. Paunov, R. Kröger and F. C. Meldrum, *Chem. Mater.*, 2013, **25**, 4994-5003.
16 S. Obara, T. Yamauchi and N. Tsubokawa, *Polym. J.*, 2010, **42**, 161-166.
17 A. Sugawara, S. Yamane and K. Akiyoshi, *Macromol. Rapid Commun.*, 2006, **27**, 441-446.
18 A.-X. Wang, D.-Q. Chu, L.-M. Wang, B.-G. Mao, H.-M. Sun, Z.-C. Ma, G. Wang and L.-X. Wang, *CrystEngComm*, 2014, **16**, 5198-5205.
19 S. Kumar, T. Ito, Y. Yanagihara, Y. Oaki, T. Nishimura and T. Kato, *CrystEngComm*, 2010, **12**, 2021-2024.
20 A. Sugawara and T. Kato, *Compos. Interfaces*, 2004, **11**, 287-295.
21 N. Hosoda, A. Sugawara and T. Kato, *Macromolecules*, 2003, **36**, 6449-6452.
22 H. Wei, N. Ma, F. Shi, Z. Wang and X. Zhang, *Chem. Mater.*, 2007, **19**, 1974-1978.
23 D. V. Okhrimenko, J. Nissenbaum, M. P. Andersson, M. H. M. Olsson and S. L. S. Stipp, *Langmuir*, 2013, **29**, 11062-11073.
24 S. Kim, S. H. Ku, S. Y. Lim, J. H. Kim and C. B. Park, *Adv. Mater.*, 2011, **23**, 2009-2014.
25 X. L. Wang, H. Bai, Y. Y. Jia, L. J. Zhi, L. T. Qu, Y. X. Xu, C. Li and G. Q. Shi, *Rsc adv.*, 2012, **2**, 2154-2160.
26 G. M. Luz and J. F. Mano, *Philos. Trans. R. Soc. A*, 2009, **367**, 1587-1605.

27 H. D. Espinosa, J. E. Rim, F. Barthelat and M. J. *Buehler, Prog. Mater. Sci.*, 2009, **54,** 1059-1100.
28 F. Liu and T. S. Seo, *Adv. Funct. Mater.*, 2010, **20**, 1930-1936.
29 H. Kumagai, R. Matsunaga, T. Nishimura, Y. Yamamoto, S. Kajiyama, Y. Oaki, K. Akaiwa, H. Inoue, H. Nagasawa, K. Tsumoto and T. Kato, *Faraday Discuss.*, 2012, **159**, 483-494.
30 D. C. Marcano, D. V. Kosynkin, J. M. Berlin, A. Sinitskii, Z. Sun, A. Slesarev, L. B. Alemany, W. Lu and J. M. Tour, *Acs Nano*, 2010, **4**, 4806-4814.
31 Z.-h. Liu, Z.-M. Wang, X. Yang and K. Ooi, *Langmuir*, 2002, **18**, 4926-4932.
32 C. Xu, X. Wang and J. Zhu, *J. Phys. Chem. C*, 2008, **112**, 19841–19845.
33 W. Zhang, W. He and X. Jing, *J. Phys. Chem. B*, 2010, **114**, 10368-10373.
34 S. Stankovich, R. D. Piner, S. T. Nguyen and R. S. Ruoff, *Carbon*, 2006, **44**, 3342-3347.
35 S. I. Kuriyavar, R. Vetrivel, S. G. Hegde, A. V. Ramaswamy, D. Chakrabarty and S. Mahapatra, *J. Mater. Chem.*, 2000, **10**, 1835-1840.
36 Z. Lin, Y. Liu and C.-p. Wong, *Langmuir*, 2010, **26**, 16110-16114.
37 Q. Shen, Y. Chen, H. Wei, Y. Zhao, D. Wang and D. Xu, *Cryst. Growth Des.*, 2005, **5**, 1387-1391.
38 H. Wei, Q. Shen, Y. Zhao, Y. Zhou, D. Wang and D. Xu, *J. Cryst. Growth*, 2005, **279**, 439-446.

CrystEngComm RSCPublishing

PAPER

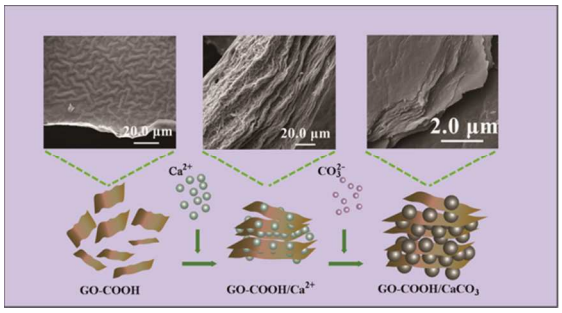

Schematic illustration for the fabrication of GO-COOH/$CaCO_3$ multi-layer hybrid structures: GO-COOH; GO-COOH /$CaCl_2$ multi-layer hybrid structure; GO-COOH /$CaCO_3$ hybrid multi-layer structure (from left to right).

highlight: Fabrication an innovative Nacre-like GO-COOH/$CaCO_3$ multi-layer hybrid structure by biomimetic mineralization process.